N,*N*′-Bis-Silylated Lithium Aryl Amidinates: Synthesis, Characterization, and the Gradual Transition of Coordination Mode from σ Toward π Originated by Crystal Packing Interactions

Sinai Aharonovich, Moshe Kapon, Mark Botoshanski, and Moris S. Eisen*

Schulich Faculty of Chemistry and Institute of Catalysis Science and Technology, Kyriat Hatechnion, Haifa, 32000, Israel

Received December 4, 2007

In this work nine lithium *N*,*N*′-bis(trimethylsilyl)amidinates−TMEDA complexes and the dimeric adduct of 2-ethylbenzonitrile lithium bis(trimethylsilyl)amide were synthesized and characterized. The later compound was found to be a kinetically stabilized intermediate in the amidinate formation. The solid state structures of the amidinates revealed several types of crystalline supramolecular structures, generated by the degree and nature of involvement of the amidinate π system in the intermolecular interactions. The π system was also found to play a significant role in the intramolecular bonding with the lithium atom. The π bonding is obtained at the expense of the σ bond, weakening it, while keeping the metal–ligand bond length almost invariable. This facile π interaction along with the Li−N σ-bond activation can imply that similar involvements of the π systems may take place in the salt metathesis reactions with these compounds.

Introduction

Lithium amidinates, $LiN(R_1)C(R_2)NR_3$, easily synthesized from the reaction of lithium amides with nitriles or organolithium compounds with carbodiimides, are useful synthons in organic and organometallic chemistry.[1] As lithium compounds they also benefit from the merits of the lithium in comparison to other heavier alkali metals, namely its high charge density which polarizes the Li−N bond and the higher solubility of its compounds in organic solvents.[2,3] Lithium amidinates serve, therefore, as reagents in the preparation of 1,3,5-triazapentadienes,[4] 1,3,5-triazines,[5,6] and bicyclic thia-aza heterocycles[7] and as intermediates in the lithium bis(trimethylsilyl)amide-catalyzed coupling of alkynes and carbodiimides.[8] These applications in addition to the wide use of lithium amidinates as ligand transfer reagents in the preparation of amidinate complexes of p, d, and f block elements[6,9–14] have raised growing interest in the last two decades in the structural study of these complexes. These studies have revealed rich and diverse coordination chemistries as expressed by the variety of the observed amidinate coordination modes, some of which are presented in Figure 1.

* Corresponding author.

(1) (a) Ostrowska, K.; Kolasa, A. In *Science of Synthesis*; Charette, A. B., Ed.; Thieme: Stuttgart, Germany, 2005; Vol. 22, p 379. (b) Ostrowska, K.; Kolasa, A. In *Science of Synthesis*; Charette, A. B., Ed.; Thieme: Stuttgart, Germany, 2005; Vol. 22, p 489.

(2) Bauer, W. In *Lithium Chemistry: A Theoretical and Experimental Overview*; Schleyer, P. v. R., Sapse, A.-M., Eds.; Wiley: New York, 1995; pp 227–293.

(3) Baldamus, J.; Berghof, C.; Cole, M. L.; Hey-Hawkins, E.; Junk, P. C.; Louis, L. M. *Eur. J. Inorg. Chem.* **2002**, 2878.

(4) Boesveld, W. M.; Hitchcock, P. B.; Lappert, M. F. *J. Chem. Soc., Dalton Trans.* **1999**, *40*, 41.

(5) Boesveld, W. M.; Hitchcock, P. B.; Lappert, M. F. *J. Chem. Soc., Perkin Trans. 1* **2001**, 1103.

(6) Volkis, V.; Nelkenbaum, E.; Lisovskii, A.; Hasson, G.; Semiat, R.; Kapon, M.; Botoshansky, M.; Eishen, Y.; Eisen, M. S. *J. Am. Chem. Soc.* **2003**, *125*, 2179.

(7) Knapp, C.; Lork, E.; Borrmann, T.; Stohrer, W.-D.; Mews, R. *Eur. J. Inorg. Chem.* **2003**, 3211.

(8) Ong, T.-G.; O'Brien, J. S.; Korobkov, I.; Richeson, D. S. *Organometallics* **2006**, *25*, 4728.

(9) (a) Edelmann, F. T. *Coord. Chem. Rev.* **1994**, *137*, 403. (b) Lu, Z.; Hill, N. J.; Findlater, M.; Cowley, A. H. *Inorg. Chim. Acta* **2007**, *360*, 1316. (c) Coles, M. P.; Swenson, D. C.; Jordan, R. F.; Young, V. G. *Organometallics* **1997**, *16*, 5183. (d) Doyle, D.; Gun'ko, Y. K.; Hitchcock, P. B.; Lappert, M. F. *Dalton Trans.* **2000**, 409. (e) So, C.-W.; Roesky, H. W.; Magull, J.; Oswald, R. B. *Angew. Chem., Int. Ed.* **2006**, *45*, 3948. (f) Green, S. P.; Jones, C.; Jin, G.; Stasch, A. *Inorg. Chem.* **2007**, *46*, 8. (g) Luo, Y.; Yao, Y.; Shen, Q.; Sun, J.; Weng, L. *J. Organomet. Chem.* **2002**, *662*, 144. (h) Zhang, Y.; Reeder, E. K.; Keaton, R. J.; Sita, L. R. *Organometallics* **2004**, *23*, 3512. (i) Thompson, D. M. U.S. Patent 2006177577, Aug. 10, 2006. (j) Decams, J. M.; Hubert-Pfalzgraf, L. G.; Vaissermann, J. *Polyhedron* **1999**, *18*, 2885. (k) Cotton, F. A.; Poli, R. *Inorg. Chim. Acta* **1988**, *141*, 91. (l) Cotton, F. A.; Ren, T. *J. Am. Chem. Soc.* **1992**, *114*, 2237. (m) Dawson, D. Y.; Arnold, J. *Organometallics* **1997**, *16*, 1111. (n) Yamaguchi, Y.; Ogata, K.; Kobayashi, K.; Ito, T. *Inorg. Chim. Acta* **2004**, *357*, 2657. (o) El-Kadri, O. M.; Heeg, M. J.; Winter, C. H. *Dalton Trans.* **2006**, 4506. (p) Wilder, C. B.; Reitfort, L. L.; Abboud, K. A.; McElwee-White, L. *Inorg. Chem.* **2006**, *45*, 263. (q) Sciarone, T. J. J.; Nijhuis, C. A.; Meetsma, A.; Hessen, B. *Dalton Trans.* **2006**, 4896. (r) Nijhuis, C. A.; Jellema, E.; Sciarone, T. J. J.; Meetsma, A.; Budzclaar, P. H. M.; Hessen, B. *Eur. J. Inorg. Chem.* **2005**, 2089. (s) Hagadorn, J. R.; Arnold, J. *Inorg. Chem.* **1997**, *36*, 132. (t) Nagashima, H.; Kondo, H.; Hayashida, T.; Yamaguchi, Y.; Gondo, M.; Masuda, S.; Miyazaki, K.; Matsubara, K.; Kirchner, K. *Coord. Chem. Rev.* **2003**, *245*, 177. (u) Singhal, A.; Jain, V. K.; Nethaji, M.; Samuelson, A. G.; Jayaprakash, D.; Butcher, R. J. *Polyhedron* **1998**, *17*, 3531. (v) Lim, B. S.; Rahtu, A.; Park, J.-S.; Gordon, R. G. *Inorg. Chem.* **2003**, *42*, 7951. (w) Wedler, M.; Noltemeyer, M.; Pieper, U.; Schmidt, H. G.; Stalke, D.; Edelmann, F. T *Angew. Chem., Int. Ed. Engl.* **1990**, *29*, 894. (x) Li, C.; Wang, Y.; Zhou, L.; Sun, H.; Shen, Q. *J. Appl. Polym. Sci.* **2006**, *102*, 22.

(10) Hitchcock, P. B.; Lappert, M. F.; Merle, P. G. *Dalton Trans.* **2007**, 585.

(11) Lisovskii, A.; Eisen, M. S. In *Topics in Organometallic Chemisty*; Marek, I., Ed.; Springer: Berlin/Heidelberg, Germany, 2005; Vol. 10, pp 63–105.

(12) Schmidt, J. A. R.; Arnold, J. *J. Chem. Soc., Dalton Trans.* **2002**, 3454.

(13) Nelkenbaum, E.; Kapon, M.; Eisen, M. S. *Organometallics* **2005**, *24*, 2645.

(14) (a) Stalke, D.; Wedler, M.; Edelmann, F. T. *J. Organomet. Chem.* **1992**, *431*, C1. (b) Villiers, C.; Thuery, P.; Ephritikhine, M. *Eur. J. Inorg. Chem.* **2004**, 4624. (c) Richter, J.; Feiling, J.; Schmidt, H.-G.; Noltemeyer, M.; Brueser, W.; Edelmann, F. T. *Z. Anorg. Allg. Chem.* **2004**, *630*, 1269.

10.1021/om701216p CCC: $40.75
Publication on Web 03/15/2008

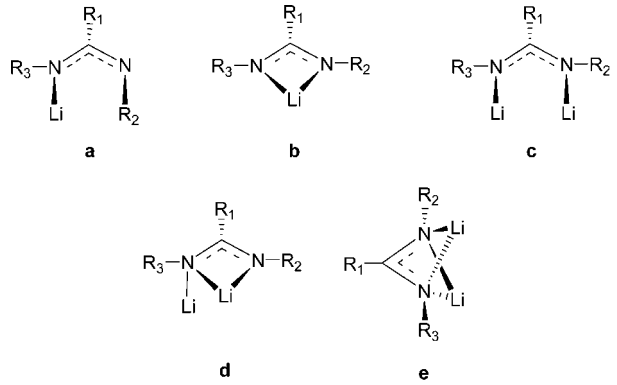

Figure 1. Examples of lithium amidinate coordination modes: (a) η^1, (b) η^2, (c) η^1:η^1 bimetallic bridging, (d) η^2:η^1 bimetallic bridging and monochelating, and (e) η^2:η^2 bimetallic bridging and bis-(chelating).

Similarly to many lithium amides and imides,[15] the nature of the coordination mode and aggregation degree between the lithium metal and a certain amidinate motif is highly affected by the presence of additional ligands or donor solvents and by the substitution of the amidinate backbone. Thus, in the presence of chelating donors such as TMEDA, the η^2 chelating mode (b in Figure 1), in which the two terminal nitrogen atoms are σ bonded to the metal, is usually observed.[3,16–19] Monochelating donors such as ether or THF may encourage the aggregation and formation of dilithium complexes with the η:$^2\eta^1$ coordination mode (d in Figure 1) in which one nitrogen is π bonded to lithium.[8,10,14,19,20] Weak monochelating σ donors such as an aromatic nitrile[21] may lead to the formation of dilithium or trilithium complexes with the η^2:η^2 (e in Figure 1) or more complex η^2:η^3 motifs, respectively, which possess a higher π bonding character.[10,17,19,22–24]

In addition to the nature of neighboring ligands in the coordination sphere, the amidinate coordination mode is also sensitive to changes in their carbon and/or nitrogen substituents. An elegant example of the large effect the different substituents of the terminal nitrogen atoms have on the coordination modes the amidinate ligands adopt was presented in a recent review by Junk and Cole on bis(aryl)formamidinates.[22]

The substituents on the central carbon are also known to affect the coordination modes and structural parameters.[25] Extremely bulky substituents such as terphenyl[18] or triptycenyl[26] may force the unusual η^1 or *Z-syn* η^1 coordination modes, respectively. Even a subtler modification on the aromatic rings in *N*,*N*′-bis(trimethylsilyl)benzamidinates results in considerable structural changes.[6,17,23] Among the amidinates, the use of the aforementioned aryl N-silylated derivatives in the chelation of transition, f-block, and main group metals is advantageous due to their facile synthesis, high crystallinity, and solubility in hydrocarbon solvents.[12] Their steric resemblance to substituted cyclopentadienyls[27] along with their lesser electron donation character and the ability to tune these properties through changes on the aromatic ring substitution promotes the use of *N*,*N*′-bis(trimethylsilyl)benzamidinates in the syntheses of group IV,[6,11,28,29] vanadium,[28,30] and nickel[13,31] complexes for catalytic olefin polymerization and other demanding chemical transformations.

To further examine the steric and the electronic effects of the central carbon substituents in *N*,*N*′-bis(trimethylsilyl)amidinates, toward the design of new early transition metal catalysts, we have prepared and characterized seven new substituted phenyl, a 2-furyl, and a 2-pyridyl derivatives. Comparison of the solid state structure of these complexes revealed similarities and differences affecting the core structural parameters that resulted even by the subtle decoration at the aromatic ring. In particular, several crystalline supramolecular structure types were identified and found to be affected by the substitution pattern. We present here how these supramolecular interactions induce a weakening of the Li−N σ bond with the concomitant strengthening of the Li−N π interaction.

Results and Discussion

We start the presentation with the syntheses and characterization of various lithium complexes including their solid state crystal structures, followed by a discussion on their supramolecular similarities and differences giving rise to unique bonding motifs.

Syntheses of the Complexes. Complexes **1**–**8** were synthesized in multigram scales by the addition of the corresponding nitriles to an equimolar hexane solution of lithium bis(trimethylsilyl)amide, $LiN(TMS)_2$, followed by the addition of an excess of TMEDA (Scheme 1).

Addition of the benzonitriles to the lithium amide in hexane, except for the *o*-methoxy derivative, afforded beige solids. This material presumably consisted of aggregates of benzamidinate and nitriles, similar to previous observations,[24] and/or $LiN(SiMe_3)_2$−nitrile dimeric adducts. These latter adducts have been

(15) (a) Armstrong, D. R.; Barr, D.; Clegg, W.; Mulvey, R. E.; Reed, D.; Snaith, R.; Wade, K. *J. Chem. Soc., Chem. Commun.* **1986**, 869. (b) Gregory, K.; Schleyer, P. v. R.; Snaith, R. *Adv. Inorg. Chem.* **1991**, *37*, 47. (c) Mulvey, R. *E. Chem. Soc. Rev.* **1991**, *20*, 167. (d) Mulvey, R. E. *Chem. Soc. Rev.* **1998**, *27*, 339. (e) Downard, A.; Chivers, T. *Eur. J. Inorg. Chem.* **2001**, 2193.

(16) (a) Dick, D. G.; Edema, J. J. H.; Duchateau, R.; Gambarotta, S. *Inorg. Chem.* **1993**, *32*, 1959. (b) Trifonov, A. A.; Lyubov, D. M.; Fedorova, E. A.; Fukin, G. K.; Schumann, H.; Muhle, S.; Hummert, M.; Bochkarev, M. N. *Eur. J. Inorg. Chem.* **2006**. (c) Cole, M. L.; Junk, P. C.; Louis, L. M. *J. Chem. Soc., Dalton Trans.* **2002**, 3906.

(17) Knapp, C.; Lork, E.; Watson, P. G.; Mews, R. *Inorg. Chem.* **2002**, *41*, 2014.

(18) Schmidt, J. A. R.; Arnold, J. *J. Chem. Soc., Dalton Trans.* **2002**, 2890.

(19) Barker, J.; Barr, D.; Barnett, N. D. R.; Clegg, W.; Cragg-Hine, I.; Davidson, M. G.; Davies, R. P.; Hodgson, S. M.; Howard, J. A. K.; Kilner, M.; Lehmann, C. W.; Lopez-Solera, I.; Mulvey, R. E.; Raithby, P. R.; Snaith, R. *J. Chem. Soc., Dalton Trans.* **1997**, 951.

(20) (a) Hitchcock, P. B.; Lappert, M. F.; Merle, P. G. *Phosphorus, Sulfur Silicon Relat. Elem.* **2001**, *168–169*, 363. (b) Pang, X.-A.; Yao, Y.-M.; Wang, J.-F.; Sheng, H.-T.; Zhang, Y.; Shen, Q. *Chin. J. Chem.* **2005**, *23*, 1193. (c) Mansfield, N. E.; Coles, M. P.; Hitchcock, P. B. *Dalton Trans.* **2005**, 2833.

(21) (a) Habeck, C. M.; Lehnert, N.; Nather, C.; Tuczek, F. *Inorg. Chim. Acta* **2002**, *337*, 11. (b) Martins, L. M. D. R. S.; Duarte, M. T.; Galvao, A. M.; Resende, C.; Pombeiro, A. J. L.; Henderson, R. A.; Evans, D. J. *J. Chem. Soc., Dalton Trans.* **1998**, 3311.

(22) Junk, P. C.; Cole, M. L. *Chem. Commun.* **2007**, 1579.

(23) Eisen, M. S.; Kapon, M. *J. Chem. Soc., Dalton Trans.* **1994**, 3507.

(24) Lisovskii, A.; Botoshansky, M.; Eisen, M. S. *J. Chem. Soc., Dalton Trans.* **2001**, 1692.

(25) Nimitsiriwat, N.; Gibson, V. C.; Marshall, E. L.; Takolpuckdee, P.; Tomov, A. K.; White, A. J. P.; Williams, D. J.; Elsegood, M. R. J.; Dale, S. H. *Inorg. Chem.* **2007**, *46*, 9988.

(26) Baker, R. J.; Jones, C. *J. Organomet. Chem.* **2006**, *691*, 65.

(27) (a) Recknagel, A.; Knoesel, F.; Gornitzka, H.; Noltemeyer, M.; Edelmann, F. T.; Behrens, U. *J. Organomet. Chem.* **1991**, *417*, 363. (b) Wedler, M.; Knoesel, F.; Pieper, U.; Stalke, D.; Edelmann, F. T. *Chem. Ber.* **1992**, *125*, 2171.

(28) Severn, J. R.; Duchateau, R.; Chadwick, J. C. *Polym. Int.* **2005**, *54*, 837.

(29) Volkis, V.; Lisovskii, A.; Tumanskii, B.; Shuster, M.; Eisen, M. S. *Organometallics* **2006**, *25*, 2656.

(30) Brussee, E. A. C.; Meetsma, A.; Hessen, B.; Teuben, J. H. *Chem. Commun.* **2000**, 497.

(31) Nelkenbaum, E.; Kapon, M.; Eisen, M. S. *J. Organomet. Chem.* **2005**, *690*, 3154.

Scheme 1. Preparation of the *N,N′* Bis(trimethylsilyl)lithium Amidinates

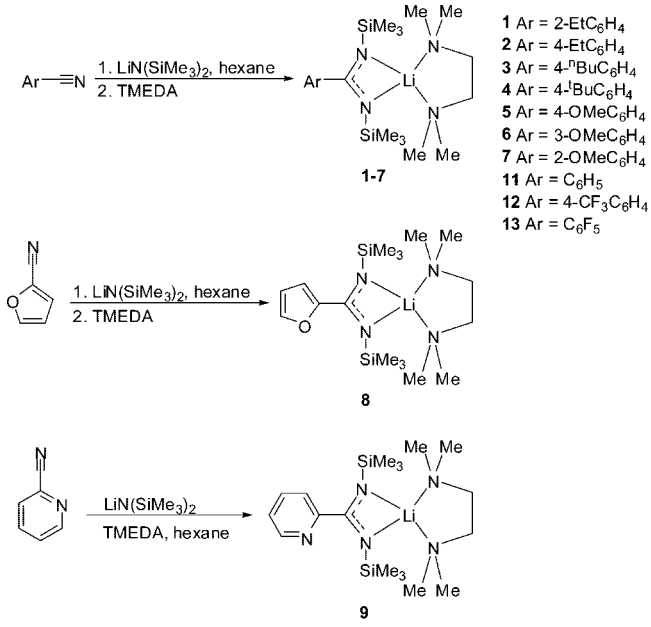

Scheme 2. Entrapment of the Dimeric LiN(TMS)$_2$-2-Ethylbenzonitrile Adduct 10 as an Intermediate in the Synthesis of Benzamidinate 1

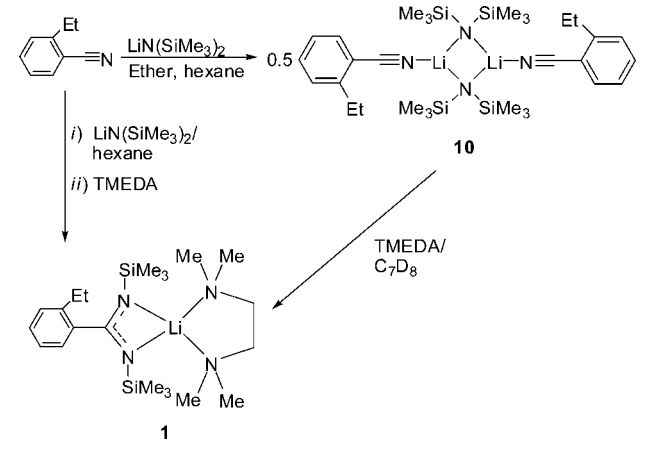

considered to be the intermediates in the reactions of amides and nitriles,[32,33] but only two of them, containing bulky aliphatic nitriles, have been crystallographically characterized.[33,34] To trap an intermediate in the reaction of the lithium amidinate with aromatic nitriles, we have performed the reaction in a more coordinative monochelating solvent, such as ether, and with the bulky ortho-substituted benzonitrile, to avoid major aggregates and to gain some kinetic stability. Hence, the addition of a hexane solution of *o*-ethylbenzonitrile to an ether slurry of LiN(SiMe$_3$)$_2$ resulted in a clear solution after stirring for 10 min at room temperature. Slow removal of the solvents from this solution yielded colorless crystals of the dimeric LiN(SiMe$_3$)−nitrile adduct **10** (Scheme 2).

The solid state structure of adduct **10** (Figure 2, Table 1), is comprised of a four-membered cyclic core, Li−N−Li−N, in which each of the trigonal planar lithium atoms is coordinated to a nitrile molecule. This core resembles the structures of many

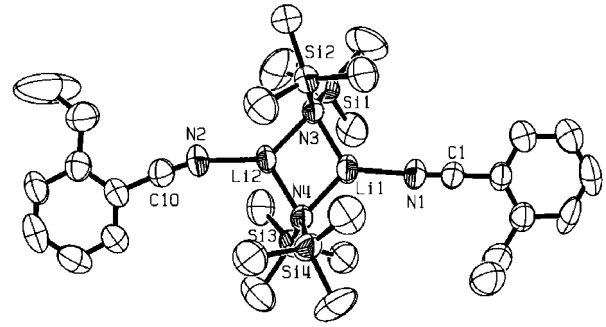

Figure 2. ORTEP diagram of the molecular structure of adduct (**10**) (50% thermal ellipsoids). Hydrogen atoms are omitted for clarity.

Table 1. Key Bond Lengths [Å] and Angles [deg] for Adduct 10

N(1)−Li(1)	2.002(8)	Li(2)−N(3)−Li(1)	74.6(3)
N(2)−Li(2)	2.016(8)	Li(1)−N(4)−Li(2)	73.9(3)
N(3)−Li(2)	1.983(8)	N(4)−Li(1)−N(3)	106.5(4)
N(3)−Li(1)	1.991(9)	N(4)−Li(1)−N(1)	128.5(5)
N(4)−Li(1)	1.978(9)	N(3)−Li(1)−N(1)	124.9(5)
N(4)−Li(2)	2.028(9)	N(3)−Li(2)−N(2)	135.4(5)
		N(3)−Li(2)−N(4)	104.9(3)
		N(2)−Li(2)−N(4)	119.6(4)
		Li(1)−N(3)−Li(2)−N(4)	0.5(0.5)

well-characterized dimeric LiN(SiMe$_3$)$_2$ adducts that differ from intermediate **10** only by the identity of the donor molecule.[35]

NMR spectroscopic measurements of a toluene-d_8 solution of crystals of **10** show a slow reaction that forms a dimeric benzamidinate complex that has a double bridging structure (**e** in Figure 1), similar to that found for the unsubstituted[6] and *p*-methyl-substituted[23] benzamidinates.

Addition of TMEDA to the aforementioned toluene-d_8 solution or to a hexane solution of **10** yielded the corresponding amidinate **1** in excellent yields. This evidence further supports that the reaction of LiN(SiMe$_3$)$_2$ with nitriles involves complexation of the lithium metal to the nitrogen of the nitrile.[24]

Unlike all the other studied benzonitriles, the reaction of 2-methoxybenzonitrile with LiN(TMS)$_2$ resulted in a clear solution after 10 h. When 2-furonitrile was added to the lithium amide, a clear red wine solution was formed gradually without any solid formation that turned faint pink after 10 h, while the reaction of 2-cyanopyridine with the lithium amide resulted in a clear yellowish solution with high viscosity and no solid

(32) (a) Koch, R.; Wiedel, B.; Anders, E. *J. Org. Chem.* **1996**, *61*, 2523. (b) Knapp, C.; Lork, E.; Borrmann, T.; Stohrer, W.-D.; Mews, R. *Z. Anorg. Allg. Chem.* **2005**, *631*, 1885.

(33) Boche, G.; Langlotz, I.; Marsch, M.; Harms, K.; Frenking, G. *Angew. Chem.* **1993**, *105*, 1207.

(34) Avent, A. G.; Antolini, F.; Hitchcock, P. B.; Khvostov, A. V.; Lappert, M. F.; Protchenko, A. V. *Dalton Trans.* **2006**, 919.

(35) (a) Boyle, T. J.; Scott, B. L. *Acta Crystallogr., Sect. C* **1998**, C54. (b) Engelhardt, L. M.; Jolly, B. S.; Junk, P. C.; Raston, C. L.; Skelton, B. W.; White, A. H. *Aust. J. Chem.* **1986**, *39*, 1337. (c) Romesberg, F. E.; Bernstein, M. P.; Gilchrist, J. H.; Harrison, A. T.; Fuller, D. J.; Collum, D. B. *J. Am. Chem. Soc.* **1993**, *115*, 3475. (d) Lucht, B. L.; Collum, D. B. *J. Am. Chem. Soc.* **1995**, *117*, 9863. (e) Lucht, B. L.; Collum, D. B. *J. Am. Chem. Soc.* **1996**, *118*, 3529. (f) Henderson, K. W.; Dorigo, A. E.; Liu, Q.-Y.; Williard, P. G. *J. Am. Chem. Soc.* **1997**, *119*, 11855. (g) Hartung, M.; Guinther, H.; Amoureux, J.-P.; Fernandez, C. *Magn. Reson. Chem.* **1998**, *36*, S61. (h) Williard, P. G.; Liu, Q. Y.; Lochmann, L. *J. Am. Chem. Soc.* **1992**, *114*, 348. (i) Armstrong, D. R.; Davies, R. P.; Dunbar, L.; Raithby, P. R.; Snaith, R.; Wheatley, A. E. H. *Phosphorus, Sulfur Silicon Relat. Elem.* **1997**, *124 & 125*, 51. (j) Lucht, B. L.; Collum, D. B. *J. Am. Chem. Soc.* **1996**, *118*, 2217. (k) Henderson, K. W.; Williard, P. G. *Organometallics* **1999**, *18*, 5620. (l) Caro, C. F.; Hitchcock, P. B.; Lappert, M. F.; Layh, M. *Chem. Commun.* **1998**, 1297. (m) Lucht, B. L.; Collum, D. B. *Acc. Chem. Res.* **1999**, *32*, 1035. (n) Forbes, G. C.; Kennedy, A. R.; Mulvey, R. E.; Rodger, P. J. A.; Rowlings, R. B. *J. Chem. Soc., Dalton Trans.* **2001**, 14. (o) Zhao, P.; Collum, D. B. *J. Am. Chem. Soc.* **2003**, *125*, 14411. (p) Godenschwager, P. F.; Collum, D. B. *J. Am. Chem. Soc.* **2007**, *129*, 12023.

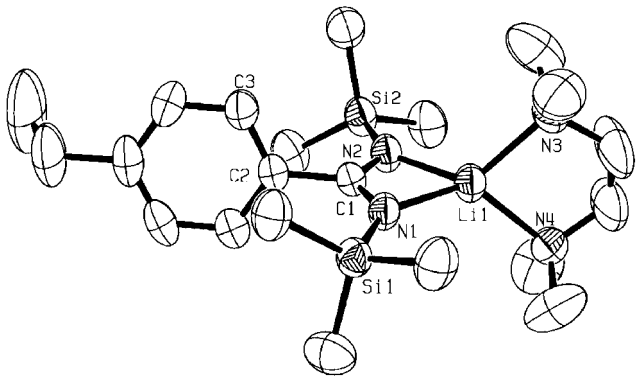

Figure 3. ORTEP diagram of the molecular structure of complex **2** (50% thermal ellipsoids). Hydrogen atoms are omitted for clarity.

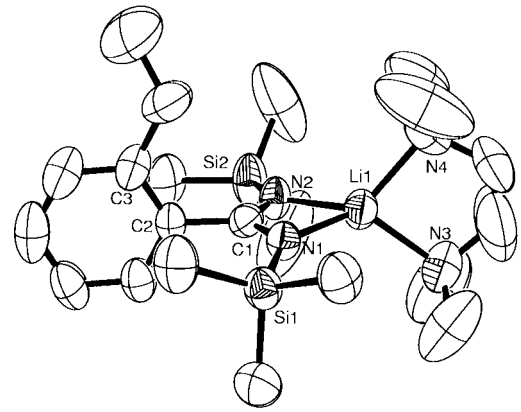

Figure 4. ORTEP diagram of the molecular structure of complex **1** (50% thermal ellipsoids). Hydrogen atoms are omitted for clarity.

formation. The lack of solid formation by the end of these reactions seems to be a net effect of a heteroatom in the vicinity of the lithium atom. This heteroatom acts as a pendant group coordinating intramolecularly with the lithium metal impeding the formation of high aggregates obviously with poor solubility in hexane. Addition of TMEDA to the reaction mixtures of any of the benzonitriles (besides the 2-cyanopyridine) yielded clear yellowish solutions of the monomeric complexes **1–8**, while a similar addition of an excess TMEDA to the viscous reaction mixture of 2-cyanopyridine resulted in a myriad of unidentified products. The desired 2-pyridyl complex (**9**) was successfully obtained by the addition of the nitrile to an equivolume TMEDA−hexane solution of $LiN(TMS)_2$. Slow cooling of the saturated hexane solutions of the complexes afforded single crystals which were characterized by X-ray diffraction studies, ^1H, ^{13}C, and 2D NMR spectroscopy, and elemental analysis.

Solid State Structure of the Complexes. The solid state structure of complexes **1–9** and those of the previously reported unsubstituted benzamidinate **11**,[6] *p*-trifluoromethylbenzamidinate **12**,[17] and pentafluorobenzamidinate **13**[17] all share a common general structure of a distorted tetrahedral central lithium atom η^2 chelated by one TMEDA and one amidinate ligand. Despite the seemingly remote site of substitution at the benzamidinate aromatic ring, various types and strengths of intermolecular forces exist in their solid state, which consecutively control the supramolecular and intramolecular structures. In addition, unique intramolecular steric effects can be created when a nonpolar ortho-substituent is present. All the studied complexes besides those containing the methoxy moiety **5–7** exhibit two types of packing arrangements in the solid state and hence we will first disclose those two supramolecular structures and then we will focus on the uniqueness of these methoxy complexes.

The Monomeric Supramolecular Structure. This packing arrangement, manifested in complexes **1**, **2**, **4**, and **12** from this work and four other published complexes,[3,36,37] corresponds to a monomeric structure in which no significant intermolecular forces that involve the amidinate core are present, as reflected by the intermolecular distance of about 4.7 Å for the above complexes. These complexes (Figures 3 and 4) also have very similar bond distances and angles (Table 2). These observations indicate that when no interactions are observed among the benzamidinate core even when there are substituent groups with various electronic and steric demands such as trifluoromethyl, *tert*-butyl, and ethyl moieties,[38] monomeric structures are obtained.

Table 2. Key Bond Lengths [Å] and Angles [deg] for Complexes 1, 2, and 4

	complex **1**	complex **2**	complex **4**
	Bond Lengths		
N(1)−C(1)	1.332(4)	1.321(3)	1.318(3)
N(2)−C(1)	1.323(4)	1.333(3)	1.318(3)
N(1)−Li(1)	2.005(7)	1.997(4)	2.009(7)
N(2)−Li(1)	2.012(7)	2.018(4)	2.009(7)
N(3)−Li(1)	2.092(7)	2.105(4)	2.096(6)
N(4)−Li(1)	2.072(7)	2.100(4)	2.096(6)
	Bond Angles		
C(1)−N(1)−Li(1)	85.0(3)	85.37(16)	84.8(2)
C(1)−N(2)−Li(1)	84.9(3)	84.19(16)	84.8(2)
N(1)−C(1)−N(2)	120.1(3)	120.36(18)	120.9(4)
N(1)−Li(1)−N(2)	69.9(2)	69.98(13)	69.6(3)
Li(1)−N(1)−C(1)−N(2)	3.5(4)	3.0(2)	0.0(4)
N(1)−C(1)−C(2)−C(3)	89.4(3)	74.9(3)	81.1(3)

Complex **1** (Figure 4) is unique in the influence the ortho-substituent has on its intramolecular bonding. The steric hindrance of the *o*-Et moiety causes the aromatic ring of this complex to be the most perpendicular to the amidinate plane, as indicated by the amidinate−phenyl dihedral angle of 89°, and forces the two TMS groups to diverge from the amidinate plane by approximately 10°. Interestingly, no additional significant intramolecular changes are observed in bond angles and distances. Regarding its supramolecular environment, the steric hindrance caused by the *o*-Et substituent is expressed in the elongation of the intermolecular distances to 5.539 and 6.070 Å, with the higher value observed at the more crowded hemisphere.

The Dimeric Supramolecular Structure. The second packing type, manifested in complexes **3**, **8** (Figure 5), **9**, and **11** is composed of dimers that contain two identical molecules. In contrast to the monomeric cases, an adjacent TMEDA methyl group (or groups) interacts directly with the amidinate core moiety disposing the intermolecular distance in the dimer motif close to 3.8 Å (Table 3). This close distance between the relatively electron poor methyl group and the electron reach amidinate core indicates the presence of a weak columbic

(36) Lee, H. K.; Lam, T. S.; Lam, C.-K.; Li, H.-W.; Fung, S. M. *New J. Chem.* **2003**, *27*, 1310.

(37) Schmidt, J. A. R.; Arnold, J. *J. Chem. Soc., Dalton Trans.* **2002**, 2890.

(38) (a) Hansch, C.; Leo, A. In *Exploring QSAR: Fundamentals and Applications in Chemistry and Biology*; American Chemical Society: Washington, DC, 1995; pp 69–76. (b) Hansch, C.; Leo, A.; Hoekman, D. *Exploring QSAR: Hydrophobic, Electronic, and Steric Constants*; American Chemical Society: Washington, DC, 1995; pp 226, 260, and 241.

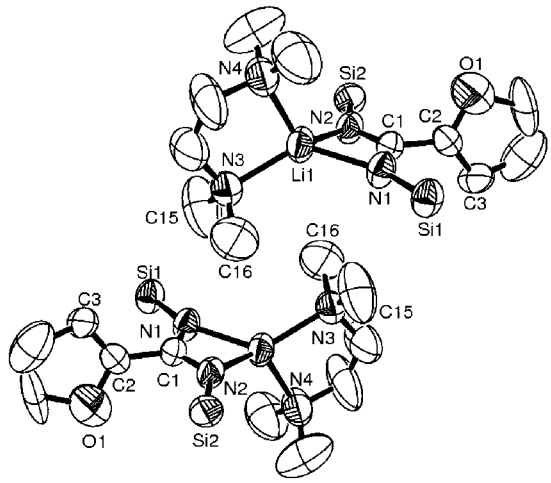

Figure 5. ORTEP diagram of complex **8**, showing a dimer (50% thermal ellipsoids). Methyl groups on silicon and hydrogen atoms are omitted for clarity.

Table 3. Key Bond Lengths [Å], Angles [deg], and Intermolecular Contact Distances [Å] for Complexes 3, 8, and 9

	complex **3**	complex **8**	complex **9**
	Bond Lengths		
N(1)−C(1)	1.330(3)	1.327(4)	1.324(2)
N(2)−C(1)	1.327(3)	1.319(4)	1.330(2)
N(1)−Li(1)	2.014(4)	2.047(7)	2.014(4)
N(2)−Li(1)	2.041(4)	2.025(7)	2.042(3)
N(3)−Li(1)	2.118(4)	2.083(7)	2.106(4)
N(4)−Li(1)	2.115(4)	2.091(7)	2.102(4)
	Bond Angles		
N(1)−C(1)−N(2)	119.94(18)	121.3(3)	120.96(17)
N(1)−Li(1)−N(2)	69.08(13)	69.0(2)	69.41(12)
Li(1)−N(1)−C(1)−N(2)	15.7(2)	7.4(2)	8.0(2)
N(1)−C(1)−C(2)−C(3)	85.8(3)	76.2(3)	62.9(2)
	Contact Distances		
C(15)−N(1)		3.756(7)	3.932(7)
C(15)−N(2)	3.683(7)		3.865(7)
C(16)−N(1)	3.728(7)		

interaction between these fragments. Interestingly, the complexes that form these dimers (besides complex **3**, which bears the *p*-^{n}Bu substituent) are those containing a small substituent at the amidinate backbone, which allows the molecules to get close. Thus, replacement of one trimethylsilyl group in the dimeric complex **11** with the bulkier 2,6-dimethylphenyl substituent[36] results in a monomeric structure for the later complex.

Dimeric and Polymeric Structures of the Methoxy Derivatives. The methoxy group in complexes **5**–**7** decorates their structural chemistry due to its involvement in intermolecular interactions. Furthermore, a change in its position at the phenyl ring promotes different supramolecular structures.

The lattice of complex **7** (Figure 6) is composed of two independent molecules with intermolecular interactions reminiscent of that of the dimeric supramolecular structures, but those interactions are formed asymmetrically. The interactions are formed by one methyl of a TMEDA molecule and one methyl of the methoxy group from the second molecule, each one having two intermolecular interactions. The TMEDA methyl group interacts with an oxygen of one methoxy group (C20b−O1a = 3.493 Å) and with the NCN core, whereas the methyl of the methoxy group interacts with the adjacent NCN core and with a collinear oxygen of the second methoxy group (O(1a)−C(8a)−O(1b) = 177.6°, C(8a)−O(1b) = 3.312 Å).

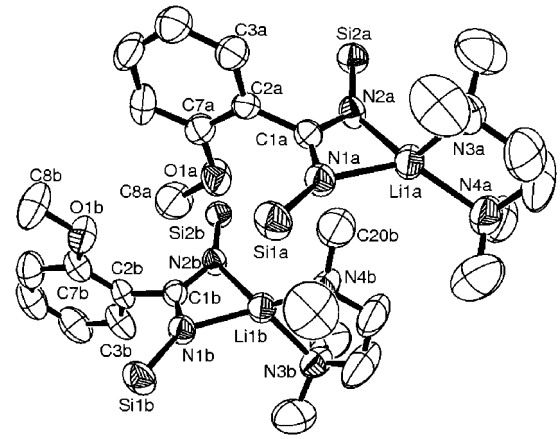

Figure 6. ORTEP diagram of the two interacting molecules of complex **7** (50% thermal ellipsoids). Methyl groups on silicon and hydrogen atoms are omitted for clarity.

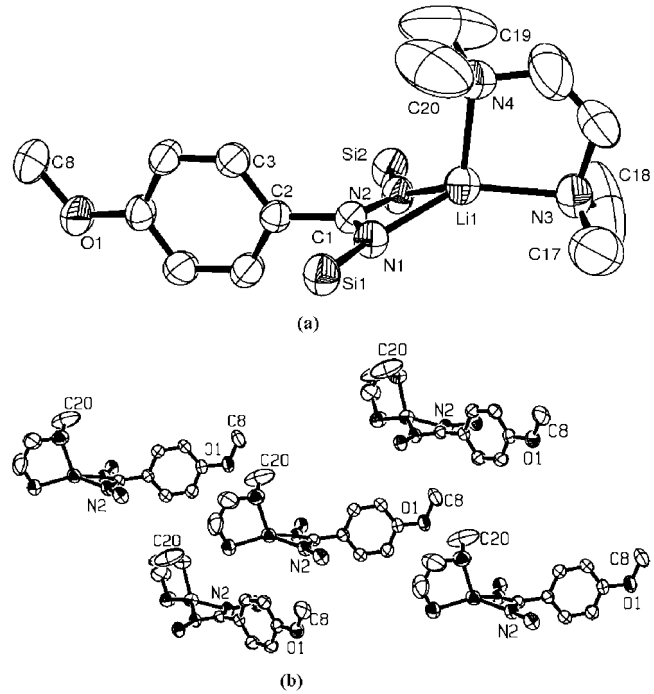

Figure 7. (a) ORTEP diagram of the molecular structure of complex **5** (50% thermal ellipsoids). Methyl groups on silicon and hydrogen atoms are omitted for clarity. (b) Intermolecular interactions of complex **5**: the central molecule interacts with four others; the interacting atoms are labeled (50% thermal ellipsoids). TMS methyl groups, TMEDA noninteracting methyl groups, and hydrogen atoms are omitted for clarity.

The supramolecular structure of complex **5** (Figure 7, Table 4) is formed by two main intermolecular interactions. Each molecule interacts with four additional molecules that have interactions with three other molecules and so forth yielding a polymeric structure. The main interactions for a central molecule are the following: The NCN core with a methoxide methyl, the TMEDA methyl with a methoxide oxygen, the methoxide and TMEDA methyls with additional NCN, and oxygen moieties of two other molecules. The four interactions to four different molecules cause complex **5** to exist as an infinite two-dimensional structure, constructed of individual sheets, each made by what can be seen as infinitely fused transoid ladders.[39]

The supramolecular structure of complex **6** (Figure 8, Table 5) defines an infinite cross-linked column structure. The column

Table 4. Key Bond Lengths [Å] and Angles [deg] for Complexes 5 and 7

	complex **7a**	complex **7b**	complex **5**
	Bond Lengths		
N(1)−C(1)	1.326(5)	1.333(5)	1.323(3)
N(2)−C(1)	1.333(4)	1.315(4)	1.337(3)
N(1)−Li(1)	2.014(7)	2.028(7)	2.017(4)
N(2)−Li(1)	2.018(8)	2.017(7)	2.025(5)
N(3)−Li(1)	2.110(10)	2.089(10)	2.091(5)
N(4)−Li(1)	2.087(9)	2.082(9)	2.106(5)
	Bond Angles		
N(1)−C(1)−N(2)	119.6(3)	120.7(3)	119.6(2)
N(1)−Li(1)−N(2)	69.5(2)	69.3(2)	69.33(16)
Li(1)−N(1)−C(1)−N(2)	10.9(5)	9.0(5)	17.3(5)
N(1)−C(1)−C(2)−C(3)	88.1(5)	86.8(5)	86.2(5)

Table 5. Selected Bond Lengthes [Å] and Angles [deg] for Complex 6

	complex **6a**	complex **6b**
	Bond Lengths	
N(1)−C(1)	1.324(6)	1.326(6)
N(2)−Li(1)	2.009(9)	2.034(9)
N(1)−Li(1)	1.997(9)	2.031(9)
N(2)−C(1)	1.323(6)	1.325(6)
N(3)−Li(1)	2.098(10)	2.090(10)
N(4)−Li(1)	2.102(9)	2.075(10)
	Bond Angles	
N(1)−C(1)−N(2)	123.0(4)	120.9(4)
N(1)−Li(1)−N(2)	71.0(3)	69.1(3)
Li(1)−N(1)−C(1)−N(2)	8.1(5)	12.0(5)
N(1)−C(1)−C(2)−C(3)	80.6(5)	88.3(5)

is formed by two independent molecules in which the methoxy group of the first interacts with the NCN core of the second. In addition, the meta hydrogen H(4b) of the second molecule interacts with one of the nitrogens of the NCN core in a third molecule that is equivalent to the first one producing the polymeric interaction (H(4b)−N(2a) = 2.89 Å, C(4b)−H(4b)−N(2a) = 168°). In addition, the methoxy group of the second molecule interacts with three different molecules (two TMEDA methylene groups and an additional methoxide oxygen) producing the cross-linkage between the columns.

It is worth mentioning that complex **13**[17] also has a polymeric structure, governed by C···F contacts in the range of 3.4–3.6 Å. All of the ring fluorine atoms participate in these interactions with TMEDA methyl and methylene, and even with TMS methyl groups.

Effect of the Packing Interactions on the Intramolecular Structures. While the participation of the amidinate π system in intermolecular interactions has a negligible effect on the N−C bond lengths (1.315−1.337 Å) and on the N−C−N bond angels (119.6−122.9°), the major influence is on the metal coordination mode, expressed in *the slippage of the Li atom and the corresponding chelating TMEDA as regards to the amidinate ligand plane.* The extent of this slippage, measured by the value of the Li−N−C−N dihedral angle, increases with the strengthening of the amidinate intermolecular interaction (Figure 9), which is evaluated by the shortest distance between an NCN core nitrogen and a carbon atom from a neighboring molecule.

Table 6. Intermolecular Contact Distances [Å] and Angles [deg] in Complexes 5−7

complex **5**	complex **6**	complex **7**
C(20)−O(1) 3.612(5)	H(4b)−N(2a) 2.89(9)	C(20b)−N(2a) 3.726(7)
C(8)−N(2) 3.579(5)	C(8a)−N(4b) 3.471(9)	C(20b)−O(1a) 3.493(7)
	O(1a)−C(8b) 3.697(9)	C(8a)−N(1b) 3.727(7)
	O(1b)−C(13a) 3.564(9)	C(8a)−O(1b) 3.311(7)
	O(1b)−C(13b) 3.582(9)	O(1a)−C(8a)−O(1b) 172.0(5)
	C(4b)−H(4b)−N(2a) 168.2(5)	

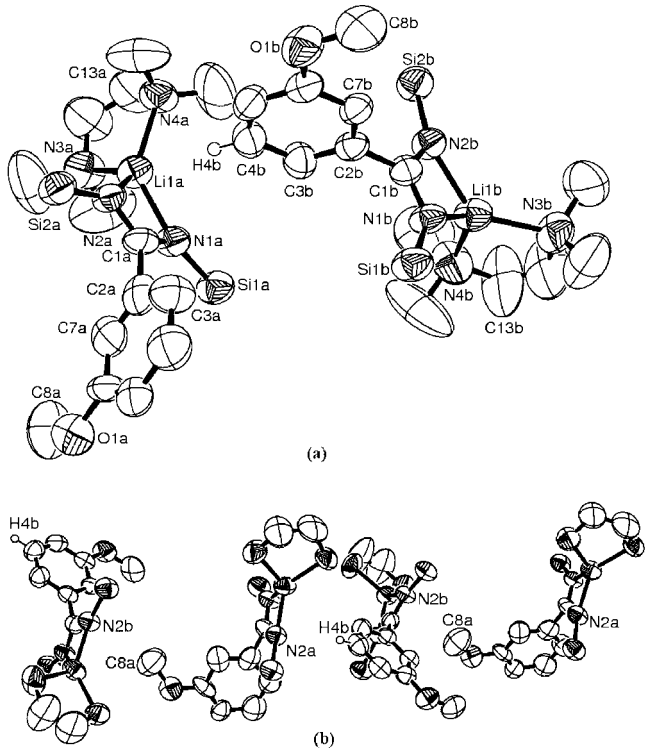

Figure 8. (a) ORTEP diagram of the molecular structure of complex **6** (50% thermal ellipsoids). Methyl groups on silicon and all noninteracting hydrogen atoms are omitted for clarity. (b) Four molecules of **6** arranged in a column, with the interacting atoms labeled (50% thermal ellipsoids). TMEDA and TMS methyl groups and all noninteracting hydrogen atoms are omitted for clarity.

The slippage of the Li atom from the NCN plane takes place in two different vectors: perpendicularly and toward the amidinate system, while the Li−N bond lengths remain unaffected (Figure 10).

In complex **5** (Figure 7a), for example, which has the largest dihedral angle, these movements are 0.596 and 0.098 Å, respectively. The TMEDA moiety, on the other hand, moves upward with the Li atom and keeps its perpendicularity with respect to the amidinate plane. It is important to point out that the Li−TMEDA distances and angles remain almost unchanged. *We suggest, therefore, that the weakening of the Li−N σ bond in the amidinate ligand, obligated from the increased angular strain, is compensated by a concurrent donation from the π system.* This shift in coordination mode is probably due to the growing degree of steric hindrance between TMEDA and the interacting fragment. Interestingly, the nitrogen in lithium anilides[40,41] also shows mixed σ/π donation to lithium. In these systems the p character in the bonding to lithium was shown to be affected by the electronic properties of the aromatic substituents as well as by intramolecular steric factors. Steric hindrance

(39) Chivers, T.; Downard, A.; Parvez, M. *Inorg. Chem.* **1999**, *38*, 4347.
(40) Bülow, R. v.; Gornitzka, H.; Kottke, T.; Stalke, D. *J. Chem. Soc., Chem. Commun.* **1996**, 1639.
(41) Bülow, R. v.; Deuerlein, S.; Stey, T.; Herbst-Irmer, R.; Gornitzka, H.; Stalke, D. *Z. Naturforsch.* **2004**, *59b*, 1471.

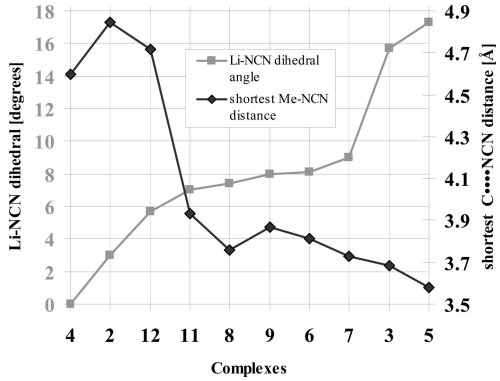

Figure 9. Opposite correlation between the intermolecular distances in complexes **2**–**9**, **11**, and **12** (◆) and the Li−NCN dihedral angle (■, degrees); complexes belonging to the monomeric category and show no significant intermolecular interactions have Li−N−C−N dihedral angles between 0 and 6°, while angles in the range of 8–18° are observed in complexes with amidinate groups that participate in intermolecular interactions.

is also believed to be responsible for similar coordination mode shifts in the β-diketiminato ligand.[42]

The amidinate ligand in complexes **1**–**13** can therefore be described as having a partially σ and partially π bonding to lithium, or in other words, that the amidinate ligand chelates the same lithium atom by using both σ and π contributions. So far, examples of η^2 or η^3 lithium amidinate with π contributions were usually restricted to dimeric and trimeric systems that lack chelating donors such as TMEDA.[6,23] For the amidinate[22] and 1-aza-allyl[41] systems these coordination modes are more common in complexes of heavier alkali metals. Similar tendency to deviate from the heteroallyl ligand plane is also observed in the alkaline earth metals in their *N*,*N*′-bis(trimethylsilyl)benzamidinato,[43] aminoiminophosphoranato,[44] and triazasulphito[45] complexes. The extent of the π bonding in these systems increases with the size, or polarizability, of the chelated metal, whereas in the later system the electronic π density was also found to play a role.

If we regard the distance of the lithium atom from the amidinate plane as a measure of the σ or π bonding degree, then the "monomeric" complexes **1**, **2**, **4**, and **12** that have the smallest Li−NCN dihedral angles and, conspicuously, also the smallest Li−NCN plane distance can be considered as predominantly σ bonded. The literature dilithium[6,23] complexes in which the latter distance is 1.36 Å can be considered as having a significant π contribution to the Li−N bond, whereas the other complexes of concern (**3**, **5**–**9**, **11**, **13**) may be seen as intermediate cases, with increasing π and weakening σ contributions with the increase of the dihedral Li−NCN angle.

The weakening of the Li−N σ bonds, facilitated by the relatively weak packing interactions, hints at their high lability, which, along with the concurrent partial chelation of the lithium by the amidinate π system, raises some conceptual questions regarding the ligand metathesis reactions of these compounds.

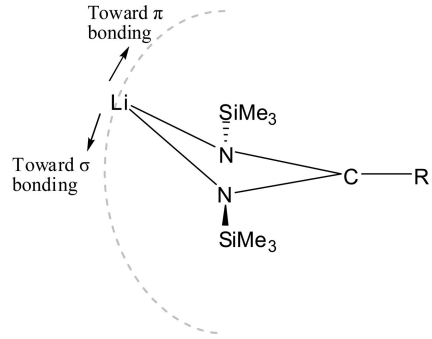

Figure 10. Slippage of the Li atom with respect to the amidinate plane. Increase in the Li−NCN dihedral angle as the π character of the bonding increases.

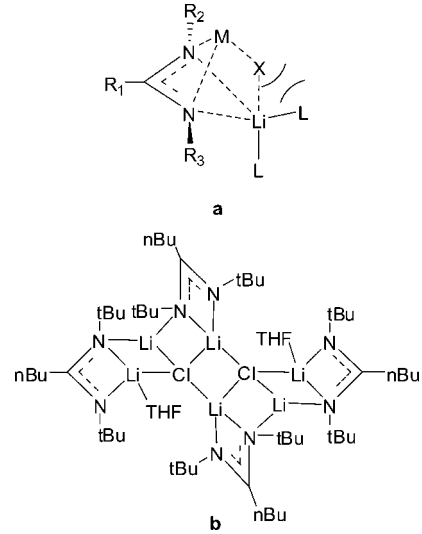

Figure 11. (a) Schematic representation of the proposed M−X and Li−N σ bond activation facilitated by the amidinate π system. (b) An aggregate of LiCl and a lithium amidinate.[39]

It is noteworthy to keep in mind that when the lithium atom slips with the TMEDA ligand it also becomes coordinatively unsaturated, hence the higher the reactivity that can be expected. As such, if a metathesis with a metal−halogen is operative it seems plausible that the halogen will interact with the lithium atom whereas the metal would π bond interact with either one or two nitrogens of the NCN core (Figure 11a). This metal, after metathesis, will slip again to the σ bonded mode as observed for early and late transition metals.[6,11,13,28–31] This proposal is supported by the existence of aggregates composed of several Li amidinate and either Li_2O,[46] LiX (X = F, Cl, Br, I, OH),[17,39] MgO,[47] or ZnO[48] units (Figure 11b). All these structures contain the structural motif of a bimetallic bonded amidinate ligand with one metal predominantly π bonded to one or two nitrogen atoms, and the other predominantly σ bonded. Both metals are also bonded to a halogen or an oxygen atom, and therefore may be considered as reflecting the proposed intermediate or transition state in the ligand metathesis reaction between a metal salt and the lithium amidinate.

(42) (a) El-Kaderi, H. M.; Xia, A.; Heeg, M. J.; Winter, C. H. *Organometallics* **2004**, *23*, 3488. (b) Bourget-Merle, L.; Lappert, M. F.; Severn, J. R. *Chem. Rev.* **2002**, *102*, 3031.

(43) (a) Neumüller, B.; Dehnicke, K. *Z. Anorg. Allg. Chem.* **2003**, *629*, 2529. (b) Westerhausen, M.; Hausen, H.-D. *Z. Anorg. Allg. Chem.* **1992**, *615*, 27. (c) Westerhausen, M.; Schwarz, W. *Z. Naturforsch.* **1992**, *47b*, 453. (d) Westerhausen, M.; Hausen, H.-D.; Schwarz, W. *Z. Anorg. Allg. Chem.* **1992**, *618*, 121. (e) Westerhausen, M.; Schwarz, W. *Z. Anorg. Allg. Chem.* **1993**, *619*, 1455.

(44) Fleischer, R.; Stalke, D. *Inorg. Chem.* **1997**, *36*, 2413.

(45) Fleischer, R.; Stalke, D. *J. Organomet. Chem.* **1998**, *550*, 173.

(46) Chivers, T.; Downard, A.; Yap, G. P. A. *J. Chem. Soc., Dalton Trans.* **1998**, 2603.

(47) Kennedy, A. R.; Mulvey, R. E.; Rowlings, R. B. *J. Am. Chem. Soc.* **1998**, *120*, 7816.

(48) Bond, A. D.; Linton, D. J.; Schooler, P.; Wheatley, A. E. H. *J. Chem. Soc., Dalton Trans.* **2001**, 3173.

Conclusions

Nine new lithium amidinate complexes were synthesized and characterized. The dimeric lithium bis(trimethylsilyl) amide 2-ethyl benzonitrilenitrile adduct was identified as a kinetically stable intermediate in the formation of the amidinate. We have found that the amidinate complexes are differentiated by the involvement degree of their π system in bonding to lithium, manifested in its deviation from the NCN plane. This involvement, which comes at the expanse of the N−Li σ bonds, is caused by the relatively weak crystalline packing forces. The substantial changes to the amidinate coordination mode inflicted by these different supramolecular arrangements and the existence of aggregates that contain lithium amidinates and metal salts indicate the plausible role of the amidinate π system in ligand metathesis reactions.

Experimental Section

General Procedure. All manipulations of air-sensitive materials were carried out with the vigorous exclusion of oxygen and moisture in oven-dried or flamed Schlenk-type glassware on a dual-manifold Schlenk line, or interfaced to a high-vacuum (10^{-5} Torr) line, or in a nitrogen-filled Vacuum Atmospheres glovebox with a medium-capacity recirculator (1–2 ppm O_2). Argon and nitrogen were purified by passage through a MnO oxygen-removal column and a Davison 4 Å molecular sieve column. Hexane, ether, and toluene-d_8 were distilled under nitrogen from Na−K alloy. TMEDA and toluene were distilled under nitrogen from Na. 2-Furonitrile was dried overnight with CaO and distilled at room temperature under reduced pressure. Lithium bis(trimethylsilyl) amide, benzonitriles, 2-cyanopyridine, and 2-furaldehyde were purchased from Aldrich and used as received. ^{1}H and ^{13}C spectra were recorded on Bruker Avance 300 and 500 spectrometers. ^{1}H and ^{13}C Chemical shifts are referenced to internal solvent resonances and reported relative to tetramethylsilane. The experiments were conducted in Teflon-sealed NMR tubes (J. Young) after preparation of the sample under anaerobic conditions, with dried toluene-d_8.

X-ray Diffraction Spectroscopy. Single crystals immersed in dry and degassed Paraton-N oil were quickly fished with a glass rod and mounted on a KappaCCD diffractometer under a cold stream of nitrogen at 230 K. Data collection and processing and structure solving were carried out with use of previously reported equipment and techniques.[6]

Syntheses. Synthesis of 2-Furonitrile. 2-Furonitrile was synthesized in high yield from 2-furaldehyde with a published method[49] and was dried and purified as described above.

Typical Procedure for Syntheses of Complexes 1–8. A frit equipped with two 100 mL flasks was charged with lithium bis(trimethylsilyl) amide (16.0–16.8 mmol) inside the glovebox. The frit was then connected to a high-vacuum line and the solids were dissolved in 30 mL of hexane. The resulted solution was cooled to 0 °C and an equimolar amount of the nitrile was added dropwise with a syringe. *p*-Methoxybenzonitrile was melted and injected with a heated syringe, resulting in the formation of solids (except for **8**). The cooling bath was removed and the mixture was kept stirring at room temperature for 3 h. TMEDA (1.5 equiv) was then added, giving an almost clear solution, which was stirred for an additional 3 h and filtered to remove solid impurities. Volatiles were gradually evaporated from the filtrate until precipitation started, and the concentrated solution was kept at −40 °C overnight to yield crystals of the product. Repetition of the crystallization process gave an additional crop of crystals.

[*o*-EtC$_6$H$_4$C(NSiMe$_3$)$_2$]Li·TMEDA (1). A 2.15 g (16.4 mmol)-sample of *o*-ethylbenzonitrile gave 5.09 g (75% yield) of **1**. ^{1}H NMR (300 MHz, toluene-d_8) δ 6.61–6.50 (m, 4H, Ph), 2.83 (q, ^3J = 3.9 Hz, 2H, CH_2-Ph), 2.04 (s, 12H, CH_3N), 1.85 (s, 4H, CH_2N), 1.44 (t, ^3J = 3.9 Hz, 3H, CH_2CH_3), 0.22 (s, 18H, CH_3Si); ^{13}C NMR (300 MHz, toluene-d_8) δ 178.1 (N−C−N), 147.6, 129.3, 128.4, 127.0, 126.3, 126.0 (Ph), 56.4 (CH_2N), 45.6 (CH_3N), 25.8 (CH_2-Ph), 14.1 (CH_2CH_3), 6.6 (CH_3Si). Anal. Calcd for $C_{21}H_{43}LiN_4Si_2$ (414.70): C, 60.82; H, 10.45; N, 13.51. Found: C, 55.91; H, 10.14; N, 12.44.

[*p*-EtC$_6$H$_4$C(NSiMe$_3$)$_2$]Li·TMEDA (2). A 2.15 g (16.4 mmol) sample of *p*-ethylbenzonitrile gave 5.43 g (80% yield) of **2**. ^{1}H NMR (300 MHz, toluene-d_8) δ 7.28 (d, ^3J = 9.0 Hz, 2H, Ph), 7.04 (d, ^3J = 6.0 Hz, 2H, Ph), 2.52 (q, ^3J = 6.0 Hz, 2H, CH_2-Ph), 2.08 (s, 12H, CH_3N), 1.89 (s, 4H, CH_2N), 1.16 (t, ^3J = 6.0 Hz, 3H, CH_2CH_3), 0.06 (s, 18H, CH_3Si); ^{13}C NMR (300 MHz, toluene-d_8) δ 179.9 (N−C−N), 145.7, 141.5, 126.8, 126.2 (Ph), 56.4 (CH_2N), 45.6 (CH_3N), 28.9(CH_2-Ph), 16.0 (CH_2CH_3), 3.3 (CH_3Si). Anal. Calcd for $C_{21}H_{43}LiN_4Si_2$ (414.70): C, 60.82; H, 10.45; N, 13.51. Found: C, 58.98; H, 10.24; N, 13.51.

[*p*-^{n}BuC$_6$H$_4$C(NSiMe$_3$)$_2$]Li·TMEDA (3). A 2.55 g (16.0 mmol) sample of *p*-*n*-butylbenzonitrile gave 6.24 g (88% yield) of **3**. ^{1}H NMR (300 MHz, toluene-d_8) δ 7.23 (d, ^3J = 9.0 Hz, 2H, Ph), 7.00 (d, ^{3}J = 9.0 Hz, 2H, Ph), 2.46 (t, ^3J = 6.0 Hz, 2H, CH_2-Ph), 2.03 (s, 12H, CH_3N), 1.84 (s, 4H, CH_2N), 1.50 (quintet, ^3J = 6.0 Hz, 2H, $CH_3CH_2CH_2CH_2$-Ph), 1.28 (sextet, ^3J = 6.0 Hz, 2H, CH_3CH_2-CH_2CH_2-Ph), 0.86 (t, ^3J = 6.0 Hz, 3H, $CH_3CH_2CH_2CH_2$-Ph), 0.05 (s, 18H, CH_3Si);^{13}C NMR (500 MHz, toluene-d_8) δ 180.2 (N−C−N), 145.8, 140.3, 127.6, 126.3 (Ph), 56.5 (CH_2N), 45.6 (CH_3N), 35.8 (CH_2-Ph), 34.1 ($CH_3CH_2CH_2CH_2$-Ph), 22.6 ($CH_3CH_2CH_2CH_2$-Ph), 14.1 ($CH_3CH_2CH_2CH_2$-Ph), 3.4 (CH_3Si). Anal. Calcd for $C_{23}H_{47}LiN_4Si_2$ (442.76): C, 62.39; H, 10.70; N, 12.65. Found: C, 57.17; H, 10.24; N, 11.70.

[*p*-^{t}BuC$_6$H$_4$C(NSiMe$_3$)$_2$]Li·TMEDA (4). A 2.55 g (16.0 mmol) sample of *p*-*tert*-butylbenzonitrile gave 6.38 g (90% yield) of **4**. ^{1}H NMR (500 MHz, toluene-d_8) δ 7.23 (dd, ^3J = 8.5 Hz, 1.1 Hz, 2H, Ph), 7.26 (dd, ^3J = 8.5 Hz, 1.1 Hz, 2H, Ph), 2.03 (s, 12H, CH_3N), 1.84 (s, 4H, CH_2N), 1.23 (s, 9H, CH_3), 0.04 (s, 18H, CH_3Si); ^{13}C NMR (500 MHz, toluene-d_8) δ 180.2 (N−C−N), 148.8, 145.5, 126, 124.3 (Ph), 56.5 (CH_2N), 45.6 (CH_3N), 34.4 (CMe_3), 31.6 (CH_3), 3.4 (CH_3Si). Anal. Calcd for $C_{23}H_{47}LiN_4Si_2$ (442.76): C, 62.39; H, 10.70; N, 12.65. Found: C, 59.04; H, 11.51; N, 12.27.

[*p*-MeOC$_6$H$_4$C(NSiMe$_3$)$_2$]Li·TMEDA (5). A 2.20 g (16.5 mmol) sample of *p*-methoxybenzonitrile gave 6.13 g (89% yield) of **5**. ^{1}H NMR (300 MHz, toluene-d_8) δ 7.28 (d, ^3J = 9.0 Hz, 2H, Ph), 7.04 (d, ^3J = 6.0 Hz, 2H, Ph), 3.23 (s, 3H, CH_3−O), 1.95 (s, 12H, CH_3N), 1.75 (s, 4H, CH_2N), 0.03 (s, 18H, CH_3Si); ^{13}C NMR (200 MHz, toluene-d_8) δ 179.9 (N−C−N), 158.4, 141.2, 127.4, 112.9 (Ph), 56.4 (CH_2N), 54.5 (CH_3−O), 45.6 (CH_3N), 3.5 (CH_3Si). Anal. Calcd for $C_{20}H_{41}LiN_4OSi_2$ (416.68): C, 57.65; H, 9.92; N, 13.45. Found: C, 53.62; H, 9.33; N, 12.67.

[*m*-MeOC$_6$H$_4$C(NSiMe$_3$)$_2$]Li·TMEDA (6). A 2.20 g (16.5 mmol) sample of *o*-methoxybenzonitrile gave 4.82 g (70% yield) of **6**. ^{1}H NMR (300 MHz, toluene-d_8) δ 7.06 (t, ^3J = 9.0 Hz, 1H, Ph), 6.88 (m, 2H, Ph), 7.06 (dd, 1H, Ph), 3.40 (s, 3H, CH_3−O), 2.02 (s, 12H, CH_3N), 1.82 (s, 4H, CH_2N), 0.04 (s, 18H, CH_3Si); ^{13}C NMR (500 MHz, toluene-d_8) δ 179.3 (N−C−N), 159.5, 149.4, 128.6, 118.9, 112.0, 111.9 (Ph), 56.4 (CH_2N), 54.5 (CH_3−O), 45.6 (CH_3N), 3.3 (CH_3Si). Anal. Calcd for $C_{20}H_{41}LiN_4OSi_2$ (416.68): C, 57.65; H, 9.92; N, 13.45. Found: C, 54.40; H, 9.46; N, 13.05.

[*o*-MeOC$_6$H$_4$C(NSiMe$_3$)$_2$]Li·TMEDA (7). A 2.20 g (16.5 mmol) sample of *o*-methoxybenzonitrile gave 5.85 g (85% yield) of **7**. ^{1}H NMR (300 MHz, toluene-d_8) δ 7.08 (dd, ^3J = 9.0 Hz, 1H, Ph), 6.95 (t, ^3J = 9.0 Hz, 1H, Ph), 6.75 (t, ^3J = 9.0 Hz, 1H, Ph), 6.46 (dd, ^3J = 9.0 Hz, 1H, Ph), 3.34 (s, 3H, CH_3−O), 1.96 (s, 12H, CH_3N), 1.78 (s, 4H, CH_2N), −0.03 (s, 18H, CH_3Si); ^{13}C NMR (500 MHz, toluene-d_8) δ 175.6 (N−C−N), 154.6, 133.7, 128.1,

(49) Talukdar, S.; Hsu, J. L.; Chou, T. C.; Fang, J. M. *Tetrahedron Lett.* **2001**, *42*, 1103.

127.0, 119.8, 110.0 (Ph), 56.5 (CH_2N), 53.8 (CH_3−O), 45.6 (CH_3N), 2.9 (CH_3Si). Anal. Calcd for $C_{20}H_{41}LiN_4OSi_2$ (416.68): C, 57.65; H, 9.92; N, 13.45. Found: C, 53.86; H, 9.48; N, 12.34.

[2-$C_4H_3OC(NSiMe_3)_2$]Li·TMEDA (8). A 1.56 g (16.8 mmol) sample of 2-furonitrile gave 5.24 g (83% yield) of **8**. ^{1}H NMR (300 MHz, toluene-d_8) δ 6.96 (dd, ^3J = 1.7 Hz, 0.6 Hz, 1H, furyl), 6.10 (d, ^3J = 2.9 Hz, 1H, furyl), 6.03 (dd, ^3J = 2.9 Hz, 1.7 Hz, 1H, furyl), 1.90 (s, 12H, CH_3N), 1.73 (s, 4H, CH_2N), 0.03 (s, 18H, CH_3Si); ^{13}C NMR (300 MHz, toluene-d_8) δ 167.9 (N−C−N), 156, 138.7, 110.3, 105.0 (furyl), 56.4 (CH_2N), 45.5 (CH_3N), 3.3 (CH_3Si). Anal. Calcd for $C_{17}H_{37}LiN_4OSi_2$ (376.61): C, 54.22; H, 9.90; N, 14.88. Found: C, 52.29; H, 9.73; N, 13.77.

[2-$C_5H_4NC(NSiMe_3)_2$]Li·TMEDA (9). A frit equipped with two 100 mL flasks was charged with 2.81 g (16.8 mmol) of lithium bis(trimethylsilyl) amide inside the glovebox. Fifteen milliliters of hexane and 15 mL of TMEDA were injected to the frit, and the resulting solution was cooled to 0 °C. Melted 2-cyanopyridine (1.75 g, 16.8 mmol) was then injected, resulting in an almost clear yellow solution. The cooling bath was removed and the solution was kept stirring at room temperature for 3 h, and then filtered to remove solid impurities. Solvents were gradually removed from the filtrate until precipitation started, and the concentrated solution was kept at −40 °C overnight to yield yellow-brown crystals of the product (4.04 g, 62% yield). ^{1}H NMR (300 MHz, toluene-d_8) δ 8.26 (s, br, 1H, H−C=N), 6.90–7.60 (s, br, 1H, pyridyl), 7.13 (t, ^3J = 6.9 Hz, 1H, pyridyl), 6.68 (ddd, ^3J = 8.7 Hz, 4.8 Hz, 1.8 Hz, 1H, pyridyl), 1.96 (s, 12H, CH_3N), 1.81 (s, 4H, CH_2N), 0.153 (s, 18H, CH_3Si); ^{13}C NMR (300 MHz, toluene-d_8) δ 148.2, 135.3, 121.3 (pyridyl), 56.5 (CH_2N), 45.6 (CH_3N), 3.3 (CH_3Si). Anal. Calcd for $C_{18}H_{38}LiN_5Si_2$ (387.64): C, 55.77; H, 9.88; N, 18.07. Found: C, 52.99; H, 9.95; N, 17.28.

{[$N(SiMe_3)_2$]Li·*o*-EtC_6H_4CN}$_2$ (10). A 826 mg (4.9 mmol) sample of lithium bis(trimethylsilyl) amide were charged in the glovebox into a frit equipped with two 50 mL flasks. The frit was connected to a high-vacuum line and 20 mL of ether was added. The resulting slurry was cooled to 0 °C and a solution of 647 mg (4.9 mmol) of the nitrile in 4 mL of hexane was added dropwise with a syringe. The cooling bath was removed and the mixture was stirred at room temperature for 10 min, after which a clear solution was obtained. Colorless crystals (1.20 g, 81% yield) of the product were obtained by gradual evaporation of the solvents. ^{1}H NMR (300 MHz, toluene-d_8) δ 7.11 (dd, ^3J = 7.8 Hz, 1.2 Hz, 2H, Ph), 6.88 (dt, ^3J = 7.8 Hz, 1.2 Hz, 2H, Ph) 6.65 (d, ^3J = 7.5 Hz, 2H, Ph) 6.59 (dt, ^3J = 7.8 Hz, 1.2 Hz, 2H, Ph) 2.56 (q, ^3J = 7.5 Hz, 4H, CH_2−Ph), 1.04 (t, ^3J = 7.5 Hz, 6H, CH_2CH_3), 0.51 (s, 36H, CH_3Si); ^{13}C NMR (300 MHz, toluene-d_8) δ 148.7 (C−Et), 133.4, 133.0, 126.4 (C−H, Ph), 118.6 (CN), 110.7 (C−CN), 27.8(CH_2−Ph), 15.1 (CH_2CH_3), 6.3 (CH_3Si). Anal. Calcd for $C_{30}H_{54}Li_2N_4Si_4$ (597.00): C, 60.36; H, 9.12; N, 9.38. Found: C, 55.09; H, 8.36; N, 8.12.

Acknowledgment. This research was supported by the USA−Israel Binational Science Foundation under contract 2004075.

Supporting Information Available: Crystallographic data for complexes **1**–**10** are available in CIF format. This material is available free of charge via the Internet at http://pubs.acs.org.

OM701216P